Vol. 354: 21–34, 2008
doi: 10.3354/meps07222

MARINE ECOLOGY PROGRESS SERIES
Mar Ecol Prog Ser

Published February 7

Phytoplankton thin layers caused by shear in frontal zones of a coastal upwelling system

J. P. Ryan[1,*], M. A. McManus[2], J. D. Paduan[3], F. P. Chavez[1]

[1]Monterey Bay Aquarium Research Institute, Moss Landing, California 95039, USA
[2]Department of Oceanography, University of Hawaii, Honolulu, Hawaii 96822, USA
[3]Naval Postgraduate School, Monterey, California 93943, USA

ABSTRACT: Using multidisciplinary observations from regional- to small-scale, we examined the development of thin phytoplankton layers in water mass frontal zones of a coastal upwelling system. Two fronts developed successively in the same region of Monterey Bay, California, USA, during August and September 2003: (1) when warm, fresh offshore waters flowed into the bay following relaxation and reversal of upwelling favorable winds, and (2) when a cold upwelling filament flowed into the bay after upwelling favorable winds resumed. Thin phytoplankton layers were observed during the presence of both fronts. The layers exhibited peaks in chlorophyll fluorescence and optical backscattering, indicating biomass maxima in the layers. Maximum chlorophyll concentrations in the layers ranged from 11 to 37 µg l^{-1} and were 4 to 55 times greater than background levels. Layer vertical thickness ranged from 1 to 5 m, averaging 2.3 m. All thin layers were in the thermocline, near the 12.5°C isotherm, and the depth of the layers varied between 12 and 33 m, in parallel with variations in thermocline depth. Synoptic mapping of the first frontal zone shortly before the thin layers developed showed strong phytoplankton patchiness. The role of vertical shear in thin layer formation from phytoplankton patches is supported by multiple results: (1) most thin layers (92%) were associated with sharp changes in the direction of horizontal currents; (2) layer thickness was significantly ($p < 0.03$) negatively correlated with shear; (3) the median shear profile, computed from all thin layer velocity profiles, peaked sharply at the center of thin layers.

KEY WORDS: Phytoplankton · Thin plankton layers · Coastal upwelling system · Shear · Thermocline

INTRODUCTION

Within many coastal regions, populations of phytoplankton are often observed in discrete thin vertical layers (Cowles et al. 1993, 1998, Dekshenieks et al. 2001, Rines et al. 2002, McManus et al. 2003). Thin phytoplankton layers typically range in thickness from a few centimeters to a few meters, and phytoplankton biomass within these layers may greatly exceed that of the rest of the water column. Development of thin phytoplankton layers may influence coastal ocean ecology in many ways, including determining patterns of primary productivity, plankton community structure, and trophic transfer, with implications for the survival of zooplankton and fish larvae, and the consequences of harmful algal blooms (Lasker 1975, Mullin & Brooks 1976, Donaghay et al. 1992, Cowles et al. 1993, 1998, Johnson et al. 1995, Rines et al. 2002, McManus et al. 2003, 2005, Koukaras & Nikolaidis 2004). Phytoplankton thin layers have been observed to extend horizontally for kilometers and to persist for days (Dekshenieks et al. 2001, McManus et al. 2003). Significant progress has been made in understanding spatial and temporal scales of thin layers and their variability relative to oceanographic forcing in some regions (e.g. McManus et al. 2003). However, there is relatively little understanding of the biological and physical processes involved in thin phytoplankton layer development across the diverse coastal environments in which they occur. This is due to the difficulty of studying thin biological layers in dynamic coastal environments.

*Email: ryjo@mbari.org

Our study site is a highly dynamic and productive coastal environment (Fig. 1). Monterey Bay, the largest open embayment along the west coast of the USA, lies in the central California Current System (CCS). Wind-driven upwelling of nutrient-rich water supports high levels of primary productivity in coastal upwelling systems like the CCS (Reid et al. 1958, Ryther 1969, Barber & Smith 1981). Coastal upwelling and its resultant enhancement of productivity have a strong seasonal dependence. In the Monterey Bay region, the climatological seasonal cycle shows upwelling and associated high productivity between March and November (Pennington & Chavez 2000). Upwelling-favorable winds from the northwest prevail during the upwelling season (Fig. 2a). However, upwelling conditions are regularly interrupted by periods of wind relaxation (Fig. 2b), when wind speed sharply decreases and wind direction can reverse. This variability in wind forcing causes rapid changes in coastal circulation and water mass distributions. Winds from the northwest generate upwelling plumes to the north and south of Monterey Bay. The plume that forms north of the bay typically flows southward across the mouth of the bay and bifurcates, such that some upwelled water flows offshore, and some flows into Monterey Bay (Rosenfeld et al. 1994). When upwelling winds relax, primary changes in the oceanography of the Monterey Bay region include increased local surface heating and rapid onshore flow of offshore waters, often in association with onshore translation of a persistent anticyclonic meander/eddy outside the bay (Rosenfeld et al. 1994, Ramp et al. 2005). The energetic mesoscale dynamics resulting from changes in wind forcing and instabilities in the CCS force rapid changes in the oceanographic conditions of Monterey Bay, which in turn force rapid and significant changes in plankton ecology.

Studies of plankton ecology require multidisciplinary observations at high spatial and temporal resolution, not only locally to detail plankton community structure and relationships to the environment, but also regionally to provide understanding of mesoscale dynamics influencing local variability (Dekshenieks et al. 2001, McManus et al. 2003, Ryan et al. 2005a,b, J. P. Ryan unpubl. data). In this contribution we integrate remote sensing from physical and bio-optical satellite sensors and shore-based HF radar mapping of surface currents with *in situ* observations from moored autonomous profilers, surface moorings, an autonomous underwater vehicle, and surface drifters to link regional scale variability in water mass distributions with small scale variability of phytoplankton thin layers. Specifically, we (1) describe the regional oceanographic variability that determined environmental conditions where the thin layers developed, (2) illustrate phytoplankton patchiness in the frontal zone,

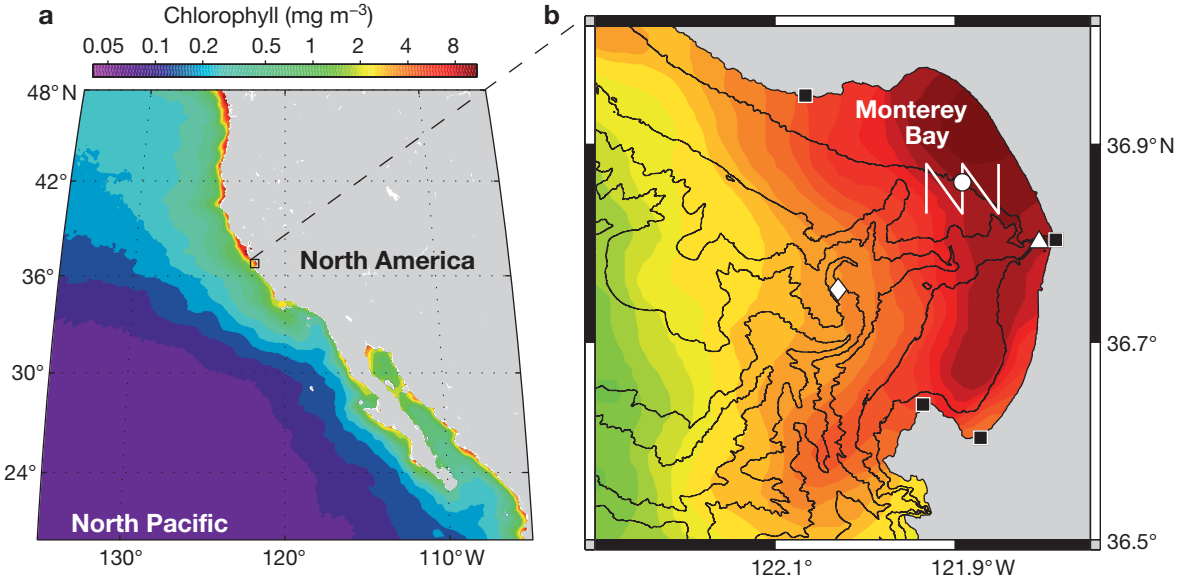

Fig. 1. Environmental setting: the productive California Current upwelling system along the eastern margin of the North Pacific Ocean. (a) Climatological mean (1998 to 2003) surface chlorophyll concentrations from the SeaWiFS satellite instrument. (b) Climatological mean SeaWiFS chlorophyll in the Monterey Bay region computed from August to September data only, 1998 to 2003 (the thin layer studies presented in this paper took place during August and September 2003). Black contours are isobaths: 50, 100, 500, 1000, 1500, and 2000 m. White symbols mark mooring locations: the ocean observatory mooring M1 (◇), a pressure sensor at the head of Monterey Submarine Canyon (△), and vertical profilers and ADCP (○). HF radar stations are indicated by ■. The white zig-zag track shows the horizontal path of repeated surveys made by an autonomous underwater vehicle

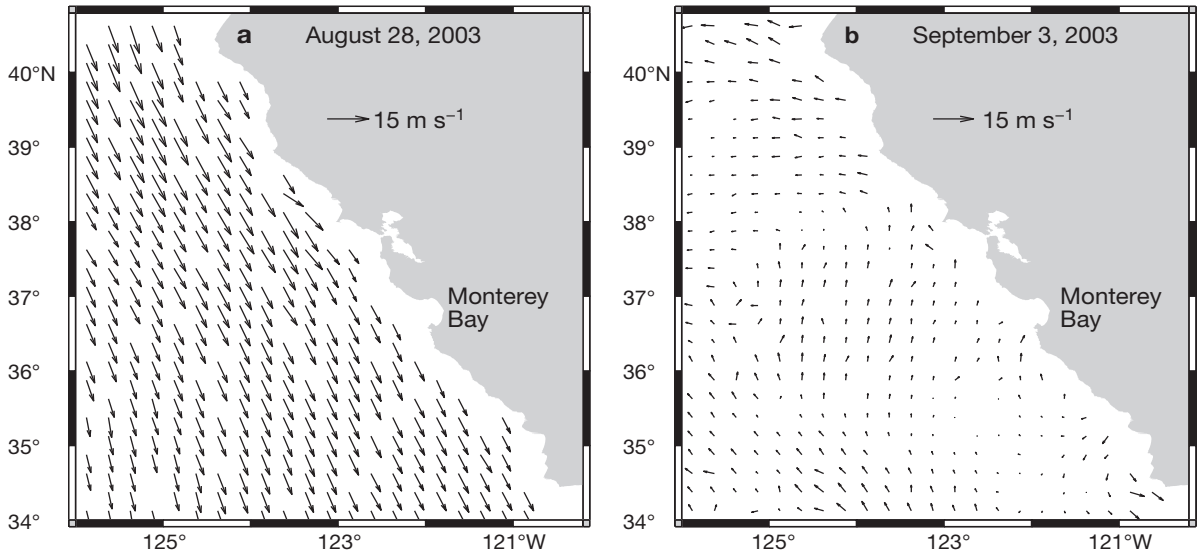

Fig. 2. Relaxation and reversal of upwelling-favorable winds. Maps show surface wind vectors over the California Current region from the SeaWinds satellite instrument during our study period: (a) upwelling-favorable northwesterly winds, and (b) a wind relaxation/reversal that occurred immediately prior to the development of thin layers in Monterey Bay shelf waters

(3) quantify attributes of the thin phytoplankton layers, and (4) support the primary role of vertical shear in the development of these thin phytoplankton layers.

MATERIALS AND METHODS

Ocean observatory mooring. An ocean observatory mooring (M1) at the mouth of Monterey Bay (diamond in Fig. 1b) monitored oceanographic and atmospheric variation in outer bay waters, and interactions between the bay and adjacent sea. Observations from M1 presented in this paper include winds, temperature, and salinity measured hourly. Surface wind speed and direction were measured by an R. M. Young model 05103 wind monitor. Temperature and salinity were measured by Sea-Bird MicroCAT conductivity, temperature, depth (CTD) sensors at 12 depths between 1 and 350 m.

Vertical profilers. To monitor water column hydrographic and bio-optical variability in northern shelf waters during 29 August to 9 September 2003, 2 autonomous vertical profilers were deployed at the 50 m isobath (circle in Fig. 1b), 95 m apart. One of the profilers, a Brooke Ocean Technology SeaHorse ('SeaHorse'), provided hourly profiles from a Sea-Bird 19 CTD and a Wet Labs WetStar fluorometer. The sensors were pumped with a Sea-Bird Electronics 5T pump. Because the fluorometer was downstream of the CTD, fluorescence measurements were aligned with temperature during post-processing, using the time-depth reference and a time lag computed from the pump flow rate and the plumbing volume between the sensors. The second profiler was a buoyancy-driven system developed by the Monterey Bay Aquarium Research Institute (MBARI), the moored vertical profiler (MVP). MVP supported a Sea-Bird 19 CTD and a WetLabs BB2F backscattering and chlorophyll fluorescence sensor. It profiled every 3 h, coincident with every third SeaHorse profile. Sensor sampling rates were 2 Hz for the SeaHorse and 0.33 Hz for the MVP. Quality of the data from the conductivity sensors on both profilers was poor. Therefore, salinity data from these sensors were not used in the study.

Acoustic doppler current profiler. To monitor water circulation at the profiler location, an RD Instruments Workhorse 300 kHz Acoustic Doppler current profiler (ADCP) was deployed in an upward-looking mode, 93 (92) m from the MVP (SeaHorse) profiler mooring. This instrument provided velocity measurements between 10 and 45 m depth at a vertical resolution of 1 m. The ADCP was configured to measure velocity profiles every 30 min, with every other profile coincident with the start of the SeaHorse profiler hourly sampling. The local magnetic declination of 14° 39′ E was specified in the configuration and thus accounted for in the computation of velocity components. The raw ADCP data were processed to u and v velocity components using RD Instruments WinADCP software. Analysis of surface current vectors from high frequency (HF) radar for September 1992 showed that the major axis of the M2 tidal ellipse at this location is oriented along the 50 m isobath (Petruncio et al. 1998). Therefore, to examine along- and cross-isobath flows relative to the layers, we rotated the coordinate system 20° clockwise to align with the local 50 m isobath (Fig. 1b).

Autonomous underwater vehicle. The MBARI autonomous underwater vehicle (AUV) 'Dorado' surveyed a volume (Fig. 1b) around the location of the moored vertical profilers and ADCP on 2 and 3 September 2003. The speed of the AUV during surveys was ~1.5 m s^{-1}, and the vehicle pitch through a sawtooth sampling pattern was 30°. These sampling attributes provided synoptic, high-resolution sections through shelf waters. The AUV was equipped with a multidisciplinary sensor suite. In this paper we present observations from 2 of the sensors essential to the description of the frontal zone and phytoplankton patchiness: a SeaBird CTD that measured temperature, conductivity, and pressure, and a HOBI Labs HS-2 sensor that measured optical backscattering at 2 wavelengths and chlorophyll fluorescence.

Drifters. To characterize local circulation patterns, we released 4 drogued drifters near the profiler moorings. The cylindrical drogues, 1 m in diameter by 5 m length and of the 'holey sock' design, spanned the depth range 2 to 7 m. They were released on 2 and 3 September and recovered on 4 and 5 September, 2003. The drifters included a control unit, GPS, instrumentation package, and telemetry system. Drifter GPS locations were recorded hourly on the drifter; for real-time tracking, GPS positions were transmitted by a Quake Global Q1500 modem designed for operating over the ORBCOMM Satellite network.

HF Radar. A network of shore-based HF radar sites has been established around Monterey Bay for the purpose of mapping ocean surface currents. These instruments use Doppler radio wave backscatter in the frequency range between 12 and 25 MHz to infer the speed of the surface waters moving toward or away from the radar site; combination of input from 2 or more radar sites allows the mapping of vector surface currents with horizontal and temporal resolution around 3 km and 1 h, respectively, out to ranges of ~50 km (Paduan & Graber 1997). Continuous surface current maps were available from 4 separate coastal HF radar sites (Fig. 1). The instruments were the CODAR SeaSonde-type HF radar systems, which rely on direction-finding techniques to determine bearing information for the backscattered ocean signals (Paduan & Graber 1997). The remotely-sensed velocity data respond directly to currents in the upper 1 m, although previous studies have shown that the vertical scale extends several tens of meters below the surface for sub-tidal-period velocity fluctuations (e.g. Paduan & Rosenfeld 1996). Errors in the HF radar-derived velocities are variable, although extensive comparisons against *in situ* observations and radar-to-radar baseline observations in Monterey Bay during this study point to uncertainty levels around 10 cm s^{-1} for the hourly velocity maps (Paduan et al. 2006). To focus on subtidal variability, we analyzed 33 h low-pass filtered currents.

Satellite remote sensing. Four sources of satellite remote sensing were used in this study, of which two were of ocean color. For the long-term climatological description of the California Current upwelling system and Monterey Bay, we used the longest available time series of satellite ocean color from the Sea-viewing Wide Field-of-view Sensor (SeaWiFS). To illustrate mean surface chlorophyll concentrations for the northeast Pacific, we averaged monthly 9 km SeaWiFS chlorophyll for the period November 1997 through December 2003. To illustrate average conditions in the Monterey Bay region during our study period of late summer, we used the mean of daily 1 km SeaWiFS chlorophyll for the months of August and September, for the years 1998 through 2003 (Fig. 1). The second source of satellite ocean color data was from the Moderate Resolution Imaging Spectroradiometer (MODIS) sensor. An advantage of MODIS is the provision of concurrent ocean color and sea surface temperature (SST) imagery; we apply this to illustrate synoptic physical and bio-optical conditions in Monterey Bay and adjacent waters during the study period. To study one of the frontal zones, we examined synthetic aperture radar (SAR) imagery from 8 September 2003, when a front and thin layers were observed in the study area. The SAR image was obtained from the Alaska Satellite Facility (ASF) and was projected from satellite to map coordinates using software from ASF. To examine the spatial structure and scale of wind relaxations during the study period, we acquired 25 km resolution wind fields measured by the SeaWinds instrument (http://poet.jpl.nasa.gov/).

Identification of thin layers. Thin phytoplankton layers were identified from chlorophyll fluorescence and optical backscatter data measured by sensors on the moored vertical profilers, using the criteria detailed by Dekshenieks et al. (2001). For a structure to be considered a thin layer, the chlorophyll profile had to meet 3 criteria. (1) The feature had to be ≤5 m thick; this is below the scale routinely sampled with bottles and nets on most oceanographic cruises. Layer thickness was measured where the optical signal was at half maximum intensity. (2) The optical signal had to be present in 2 or more sequential profiles. (3) The optical signal had to be at least 3 times greater than background. These criteria are conservative and effectively eliminate ephemeral features (Dekshenieks et al. 2001). Because the temporal resolution of the SeaHorse was 3 times greater than that of the MVP, layer statistics were computed from the SeaHorse data. Because bio-optical sensing from the MVP provided concurrent fluorometric chlorophyll

and optical backscatter, these data were used to determine whether the chlorophyll fluorescence maxima of the layers were true biomass maxima.

RESULTS

Responses to wind variability

The observations presented in this paper were made during August and September 2003. During this period, winds were predominantly from the NW, upwelling favorable (Fig. 3a). Five wind relaxation events occurred during this period, and each wind relaxation was accompanied by reversal of the alongshore winds. Consistent oceanographic responses to wind variability were observed in outer Monterey Bay at M 1 (location shown in Fig. 1). Wind relaxations can result in warming of surface waters through local heating and/or onshore flow of warmer offshore waters. Waters are also typically fresher offshore, therefore, the appearance of low salinity waters can be used to identify onshore flow in response to wind relaxation. All wind relaxation periods in August and September 2003 were followed by significant warming through the upper 100 m at the mouth of the bay, and 4 of the 5 relaxation events showed significant salinity decreases indicative of onshore flow (Fig. 3b,c). Variability in the timing and magnitude of oceanic responses is evident in the different relaxation events. Response variability may result from differences in the strength and nature of each wind relaxation, as well as variation in the background water mass distributions and mesoscale structures (filaments and eddies) that are present when the relaxation occurs.

During the moored profiler deployment, 29 August to 9 September (shaded period in Fig. 3), winds varied from upwelling favorable, to relaxed/reversed, and back to strongly upwelling favorable. The wind relaxation was strongly developed by 31 August, when wind speeds dropped to near zero (Fig. 3a), and the peak of the wind reversal occurred on 3 September (Figs. 2b & 3a). During and following the wind relaxation and reversal, local warming and freshening occurred at M1, indicating onshore flow of offshore waters (Fig. 3b,c). Decreasing temperature and increasing salinity were evident by 7 September, indicating the influence of upwelling following the transition back to upwelling favorable winds (Fig. 3a–c).

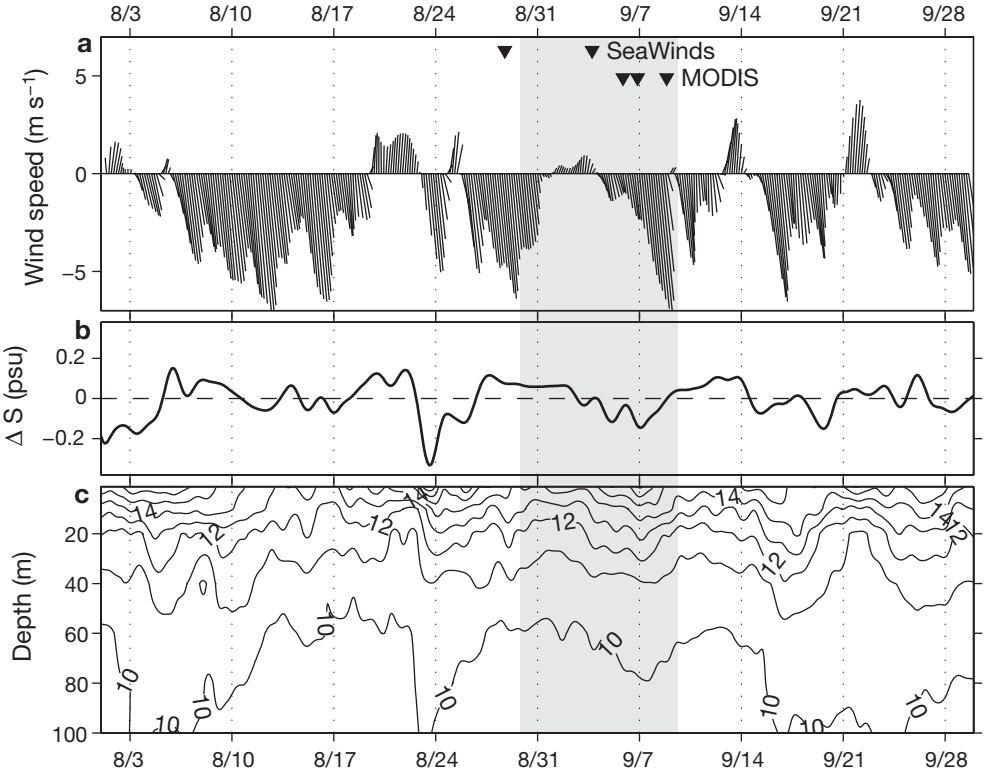

Fig. 3. Relationships between wind forcing and oceanic variability at mooring M1 (location shown in Fig. 1b). (a) Vectors showing the direction and magnitude of the wind speed. Black triangles mark the times of satellite observations. (b) Surface salinity anomaly. (c) Temperature (isotherms, °C) in the upper 100 m. All time series were 33 h low-pass filtered, except the salinity anomaly time series which was band-pass filtered for the range 33 h to 15 d. The shaded period was when the vertical profilers and ADCP were operational in northern shelf waters (location shown in Fig. 1b). Dates are month/day

Development of fronts in the bay

Intrusion of offshore waters into the bay following the wind reversal was first imaged by MODIS on 5 September. Warm, low-chlorophyll offshore waters were flowing shoreward over the southern half of the bay, forcing cooler, chlorophyll-rich resident bay waters seaward over the northern half of the bay (Fig. 4a,d). Drifters released at the profiler mooring site on 2 September flowed northwestward out of Monterey Bay during 2 to 5 September (Fig. 4a). By 5 September, the profiler moorings resided in a frontal zone between chlorophyll-rich, cool bay waters to the north and chlorophyll-poor, warm intrusion waters to the south. The nearest clear MODIS imagery of the region prior to 5 September was from 23 August. This gap in satellite coverage precludes remote sensing description of the earlier phase of response to the wind relaxation.

Synoptic mapping of the region around the profilers on 2 and 3 September allowed examination of the earlier phase of water mass intrusion and scales of phytoplankton patchiness in the frontal zone (Fig. 5). The AUV surveys on consecutive days showed warming and freshening of the upper water column associated with the intrusion of offshore waters (Fig. 5a,b,e,f). The lowest salinity waters were intruding below the surface (Fig. 5b,f). The profilers were evidently in a region of strong horizontal gradients and tilting isotherms and isohalines associated with the water mass frontal zone. Chlorophyll fluorescence and optical backscatter revealed highly patchy phytoplankton distributions (Fig. 5c,d,g,h). The spatial patterns in optical backscatter were similar to those in chlorophyll fluorescence, indicating that the fluorescence maxima of the upper water column were biomass maxima. Horizontal scales of the patches having high chlorophyll fluorescence and optical backscatter were ~1 to 3 km. None of the AUV profiles through the phytoplankton patches on 2 to 3 September met the thin layer criteria. In the shallowest segment of the surveys, strong optical backscattering plumes having low chlorophyll fluorescence extended from the bottom to near surface (Fig. 5c,d,g,h). These plumes were likely bottom sediments being mixed/transported into the shallow pelagic environment.

Water mass and frontal distributions on 6 September were very similar to those observed on 5 September (Fig. 4a,b,d,e). The return of upwelling favorable winds following the wind relaxation and reversal (Fig. 3a) caused significant changes in water mass distributions around the profiler mooring site. By 8 September, a filament of recently upwelled water extended into the bay from the north, bringing relatively cool, high-chlorophyll waters along the western side of the profiler mooring site (Fig. 4c,f). Multi-platform radar observations from 8 September indicate that these changes brought a convergent frontal zone directly over the profiler mooring site (Fig. 6). The dark regions of the SAR image indicate a relatively smooth sea surface, which can be caused by buoyant matter that accumulates in convergence zones and dampens surface roughness (Thompson & Gasparovic 1986). This is supported by the convergence field computed from HF radar currents, which shows maximum convergence aligned with the dark areas of the SAR image (hatched regions in Fig. 6).

Local environment and attributes of phytoplankton thin layers

The moored profilers observed oceanographic responses to wind variability and the development of thin layers in the water column. The profiler deployment period coincided with a transition from a nearly equal, semidiurnal neap tide to an unequal, semidiurnal spring tide (Fig. 7a). The surface layer warming following wind relaxation that was mapped by AUV on 2 to 3 September (Fig. 5) was measured by the vertical profiler (Fig. 7b). Diurnal vertical excursions of the thermocline of ~10 m began on 5 September and persisted through 9 September (Fig. 7b). The isotherm depression phase of this cycle coincided with the second flood tide of the unequal semidiurnal tide (Fig. 7a,b).

A sharp decrease in chlorophyll was first observed on 2 September (Fig. 7c), indicating that the initial arrival of lower chlorophyll offshore waters occurred on that day. Thin phytoplankton layers were first observed on 6 September (Fig. 7a,c), when the first frontal zone was still present at the mooring site (Fig. 4b,e). The layers were consistently near the 12.5°C isotherm during day and night, and their depth changed significantly over short time scales, in parallel with the vertical movement of the thermocline. On 6 and 7 September, the layers were only observed during the second flood tide of the semidiurnal cycle and its adjacent slack periods (Fig. 7a). By 8 September, there was no relationship between thin layer presence and phase of the tidal cycle. This change coincided with a change in the nature of the frontal zone around the profiler moorings as an upwelling filament flowed west of the profilers (Fig. 4c,f), and a convergent front resided over the profiler mooring site (Fig. 6).

Thin layer attributes for each layer observed by the SeaHorse profiler are presented in Table 1. Of the 65 hourly profiles measured during the period of thin layer observations, 36 (55%) showed the presence of a thin layer. Layer thickness ranged from 1 to 5 m with

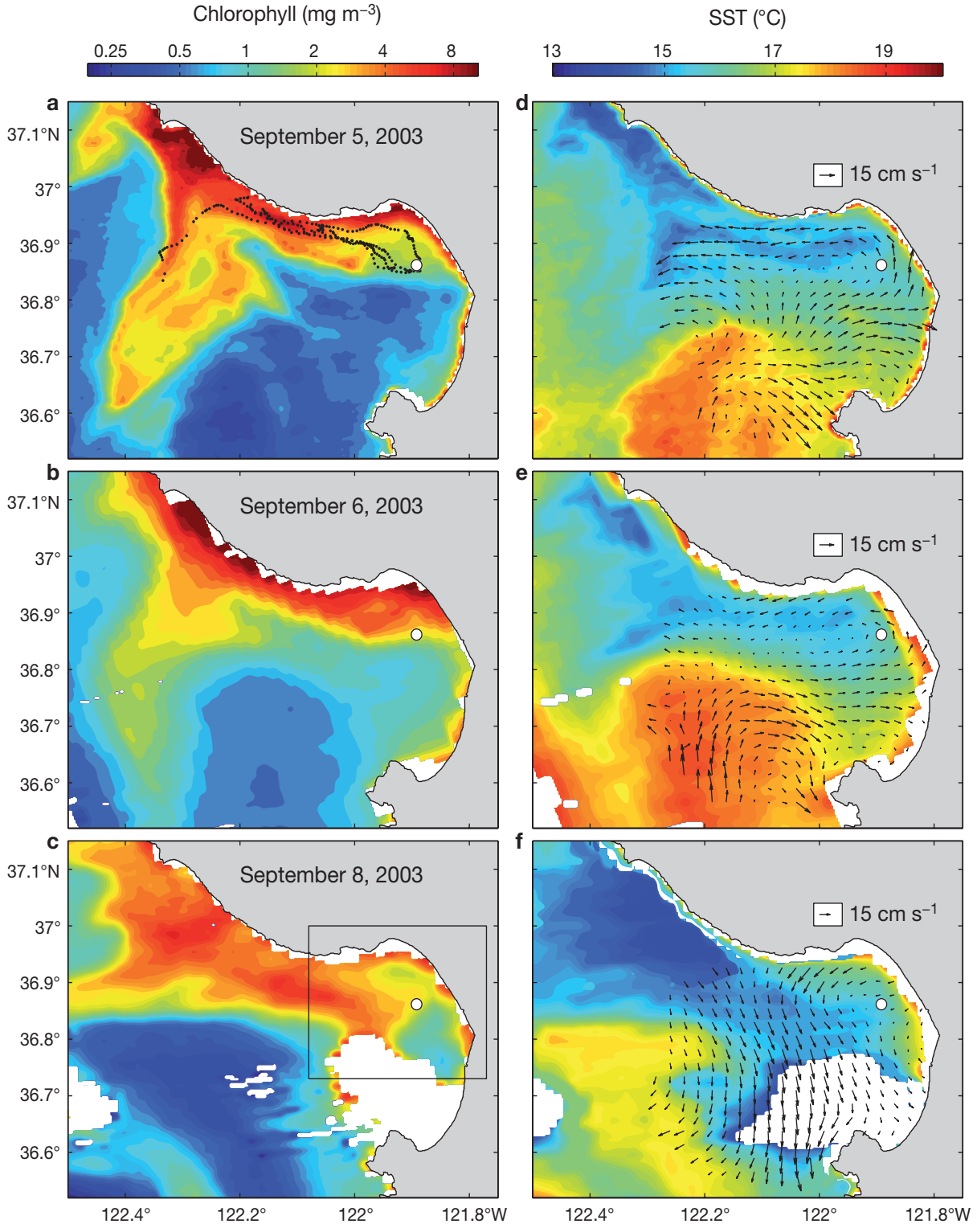

Fig. 4. Water mass changes and frontal zone development following changes in wind forcing. Shown are concurrent images of (a–c) surface chlorophyll concentrations and (d–f) sea surface temperature (SST) from the MODIS satellite sensor. Daily average HF radar surface current vectors are overlaid on the SST images. Surface drifter tracks for 2 through 5 September are overlaid on the 5 September chlorophyll image to illustrate the flushing of chlorophyll-rich waters from the bay. Drifters were released around the profiling mooring site (O) and were transported NW and out of the bay. The box in (c) shows the domain of the synthetic aperture radar (SAR) image presented in Fig. 6

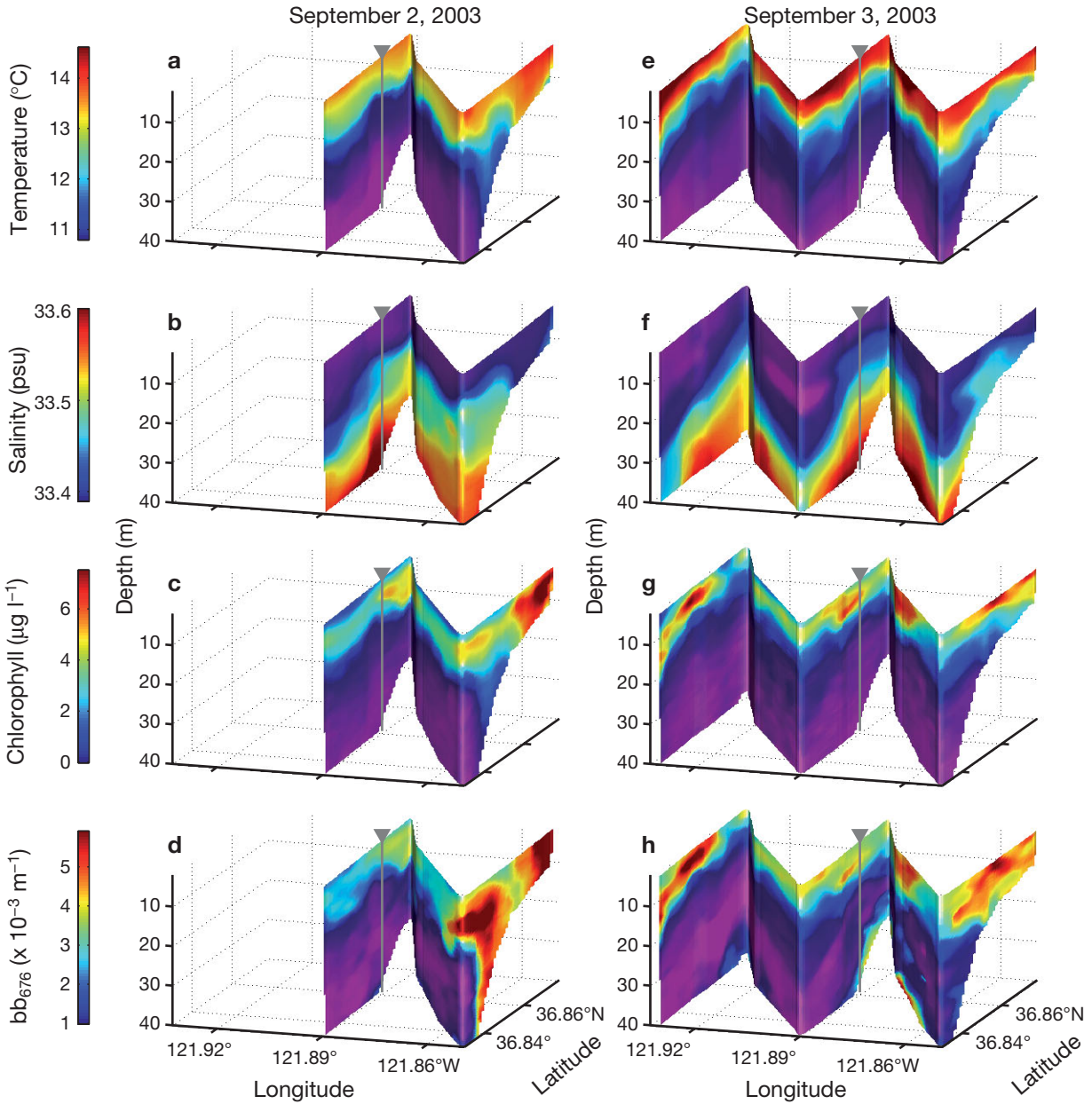

Fig. 5. Evolution of the frontal zone mapped by an autonomous underwater vehicle (AUV). The AUV survey track is shown in Fig. 1b. The zonal and meridional scales of the survey domain are 7.5 and 5.3 km, respectively. The vertical sections of hydrographic and optical properties were mapped on 2 and 3 September 2003. The location of the profiler moorings along the central transect is shown (▼). The partial survey on 2 September included 76 profiles made along the survey track in 3.5 h. The full survey on 3 September included 110 profiles completed in 5.5 h. bb_{676}: optical backscattering at 676 nm

an average of 2.3 m; most (89%) were 3 m or thinner. Quantified from chlorophyll fluorescence profiles, layer intensity ranged from 4 to 55 times greater than the background, with an average of 14 times greater. Maximum chlorophyll concentrations in the layers ranged between 11 and 37 µg l^{-1}. Chlorophyll fluorescence and optical backscatter were measured concurrently on the MVP. These data show that for all thin layers observed by this profiler, chlorophyll fluorescence maxima of the thin layers coincided with local maxima in optical backscatter (Fig. 8). Thus, the layers were true biomass maxima.

The thin layers showed consistent associations with local hydrographic conditions and velocity profiles. Of all thin layer profiles, 77% resided within a zone of relatively steep thermal gradient, bordered above, and

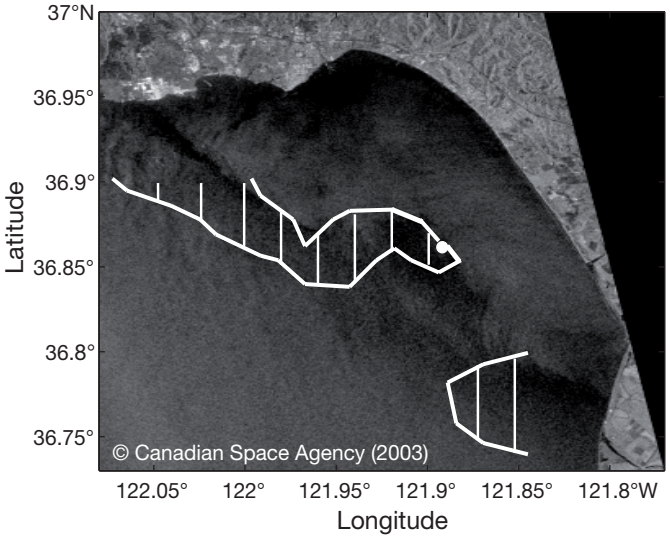

Fig. 6. Physical characterization of the second frontal zone from radar remote sensing. The image is synthetic aperture radar (SAR) from 8 September 2003, 02:00 h Greenwich Mean Time. The white hatched contours mark the zones of maximum convergence in surface flows (>9×10^{-6} s^{-1}), computed from a 12 h average of HF radar 33 h low-pass filtered surface velocity. The white circle shows the location of the profiler moorings in the frontal zone

often also below, by zones of relatively low temperature gradients. A sequence of hourly temperature and chlorophyll profiles illustrates the relationship of thin layers with steps in the thermocline at which vertical temperature gradients were enhanced (Fig. 9). In this sequence, appearance of thin layers coincided with the arrival of multiple steps in the thermocline, with the layer on the deepest step (Fig. 9a–g). Broadening and disappearance of thin layers coincided with weakening and disappearance of the stepped structure in the thermocline (Fig. 9h–l). This layer variability occurred when the upwelling filament front was in the profiler region (Figs. 4c,f & 6).

Relationships between thin phytoplankton layers and shear

Velocity profiles showed that most layers were located within or adjacent to a sharp change in the direction of horizontal velocity. Examples of this structure are shown in Fig. 10. Of all thin layer profiles, 91% were observed in direct coincidence with a reversal in the direction of along and/or cross-shelf flow. A

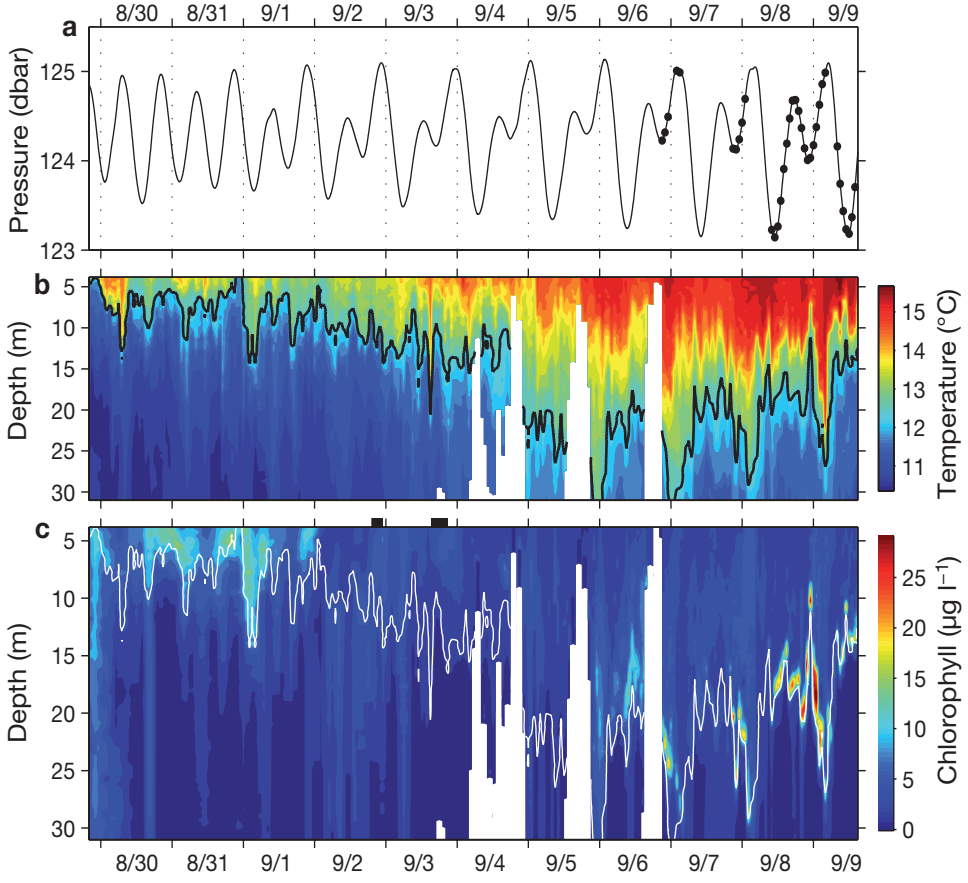

Fig. 7. Tidal and water column variability during the period of water mass changes and thin layer development in frontal zones. (a) Bottom pressure at the head of Monterey Canyon (Fig. 1b), 3 h low-pass filtered; bottom pressure variation at the profiler mooring site was in phase with this record. (b) Water column temperature at the profiler mooring site; this location is shown relative to surface and water column variability in Figs. 4–6. (c) Water column chlorophyll concentrations at the profiler mooring site. The black contour in (b) and the white contour in (c) are the 12.5°C isotherm. The white spaces in (b) and (c) are due to incomplete descent of the SeaHorse profiler to bottom between ascending data acquisition profiles. The black dots in (a) indicate thin layer encounters relative to the tidal cycle. The black bars along the top axis of (c) indicate the times of the AUV surveys shown in Fig. 5. Dates are month/day

Table 1. Dates and times of thin layer observations, layer attributes, and mean shear squared in the depth range of each thin layer. Day is of September 2003. BG: background chlorophyll concentration of the thin layers, Intensity: maximum chlorophyll concentration in the layer, Intensity factor: (Intensity–BG)/BG, Lower and Upper: depths of the thin layer boundaries, S^2: shear squared; the missing value is due to incomplete resolution of velocity within the layer depth range

Day	Time	BG ($\mu g\ l^{-1}$)	Intensity ($\mu g\ l^{-1}$)	Intensity factor	Lower (m)	Upper (m)	Thickness (m)	S^2 ($\times 10^{-4}\ s^{-2}$)
6	2100	1.9	14.2	6.5	23.0	25.0	2.0	5.3
6	2200	1.9	22.3	10.8	24.0	26.8	2.8	1.99
6	2300	1.9	21.5	10.4	26.0	28.0	2.0	0.86
7	0200	1.9	14.0	6.4	27.0	30.0	3.0	1.04
7	0300	1.9	10.6	4.6	30.0	32.8	2.8	2.66
7	2100	2.6	27.6	9.5	23.0	24.0	1.0	0.37
7	2200	1.9	23.6	11.5	27.0	30.0	3.0	0.6
7	2300	1.9	21.9	10.6	21.8	24.0	2.2	1.09
7	2400	2.6	20.5	6.8	24.0	26.0	2.0	5.25
8	0100	2.6	21.2	7.0	24.0	25.8	1.8	5.47
8	1000	1.5	13.9	8.2	22.0	24.2	2.2	3.08
8	1100	1.5	17.0	10.2	19.8	22.0	2.2	2.29
8	1200	1.5	21.3	13.0	20.0	22.0	2.0	7.11
8	1300	1.5	22.7	14.0	19.0	21.5	2.5	0.91
8	1400	1.2	16.6	13.4	17.9	19.5	1.6	3.76
8	1500	1.5	19.4	11.8	16.5	19.0	2.5	1.64
8	1600	1.9	22.0	10.7	20.0	22.0	2.0	5.85
8	1700	1.5	25.2	15.6	19.5	21.0	1.5	9.17
8	1800	1.2	17.1	13.9	19.5	21.0	1.5	9.96
8	1900	0.4	23.1	55.1	19.0	21.2	2.2	8.96
8	2000	1.2	25.7	21.4	22.0	24.0	2.0	1.7
8	2100	1.2	27.1	22.5	21.0	24.0	3.0	4.01
8	2200	1.9	36.6	18.4	17.5	19.8	2.3	13.24
8	2300	1.2	29.9	25.0	12.0	14.4	2.4	
8	2400	3.4	30.0	7.9	18.0	23.0	5.0	3.26
9	0100	2.6	36.6	12.9	19.5	24.0	4.5	0.81
9	0200	2.6	28.9	10.0	23.0	28.0	5.0	3.67
9	0300	1.9	20.4	9.8	23.0	27.0	4.0	1.92
9	0400	3.4	18.1	4.4	29.0	31.0	2.0	5.4
9	0800	0.4	16.0	38.0	15.3	16.5	1.2	7.76
9	0900	1.2	16.5	13.3	18.0	20.0	2.0	4.78
9	1000	1.2	24.3	20.1	16.7	19.0	2.3	6
9	1100	1.2	22.3	18.4	13.5	15.0	1.5	18.46
9	1200	1.2	17.1	13.8	15.5	17.5	2.0	7.87
9	1300	1.5	17.5	10.5	16.0	17.0	1.0	11.32
9	1400	1.2	18.5	15.1	15.4	16.8	1.4	0.84
Mean		1.7	21.1	13.8	20.0	22.2	2.3	4.68

similar relationship was observed for zooplankton layers and current flow in Monterey Bay (McManus et al. 2005). Thin phytoplankton layer thickness was significantly negatively correlated with average shear computed over the depth range of each layer ($p < 0.03$). Thinner layers corresponded to higher shear; thicker layers were associated with lower shear. Lastly, the median profile of shear, computed from all thin layer profiles over the depth range ±5 m of the center of each thin layer, exhibited a distinct peak centered on the thin layers (Fig. 11). These analyses support the central role of shear in the development of these thin layers.

DISCUSSION

Thin phytoplankton layers may form by diverse processes. Donaghay et al. (1992) showed that in a permanently stratified estuary, thin layers can develop with species vertical zonation patterns due to *in situ* growth and photoadaptation. Extensive observations of a dense population of *Akashiwo sanguinea* in Monterey Bay has shown that swimming of motile phytoplankton can produce thin layers as phytoplankton aggregate on the nutricline (Donaghay et al. 2006). Modeling studies have shown that phytoplankton thin layers can result from interaction of plankton motility and inter-

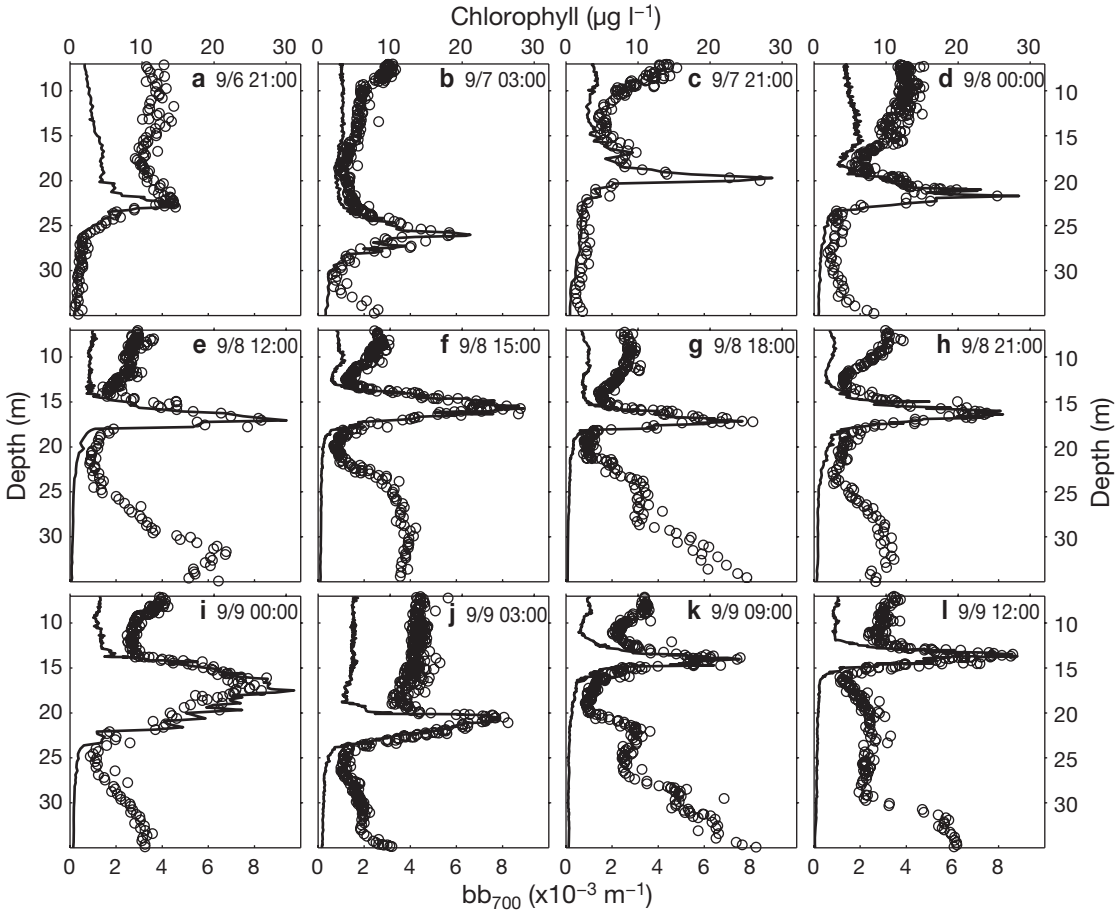

Fig. 8. Evidence that the chlorophyll fluorescence maxima of the thin layers were biomass maxima. The sequence shows chlorophyll fluorescence (—) and optical backscatter at 700 nm (bb$_{700}$, O) for all thin layer profiles from the moored vertical profiler (MVP). Sparse coverage of sharp layer gradients in a few profiles was due to a relatively slow sampling rate for the sensors on MVP. The month/day and hour of each profile is noted

nal tidal currents (Kamykowski 1974), and vertical shear in horizontal currents acting upon phytoplankton patches (Franks 1995). Studies of East Sound, Washington, a small fjord of Orcas Island, have shown that thin layers are frequently recurring features of the ecosystem, and that stratification, shear, and regional water mass variability all influence the development and evolution of the thin layers (Dekshenieks et al. 2001, Rines et al. 2002, McManus et al. 2003).

Among thin layer generation mechanisms, our data address both biological and physical processes. Because the thin layers were observed to remain in the thermocline near the 12.5°C isotherm through day and night, diurnal vertical migration is not indicated as a mechanism that caused these observed thin layers. Among the possible physical mechanisms, we find strong support for shear acting upon phytoplankton patches. Shear can create vertical gradients from horizontal gradients as waters of different properties are stirred across fronts (Eckart 1948). In this process the vertical scale of a patch is reduced as vertical shear displaces fluid differentially over the depth range of the patch. This mechanism was explored in a modeling study of phytoplankton thin layer formation by near-inertial wave shear, and it is expected to be most effective in frontal zones where horizontal gradients of phytoplankton biomass are strong (Franks 1995). Our synoptic mapping of the first frontal zone indicated very strong patchiness in the phytoplankton populations on horizontal scales of ~1 to 3 km. The role of shear acting upon phytoplankton patches was supported by multiple results: the coincidence of the thin layers with interfaces where horizontal current vectors changed sharply, the significant correlation between layer thickness and shear, and the statistics of the shear profiles computed in the layer frame of reference. Although the thin layers were associated with vertical shear, the thermocline must have been sufficiently stable to suppress turbulent vertical mixing that would dissipate the layers (McManus et al. 2003).

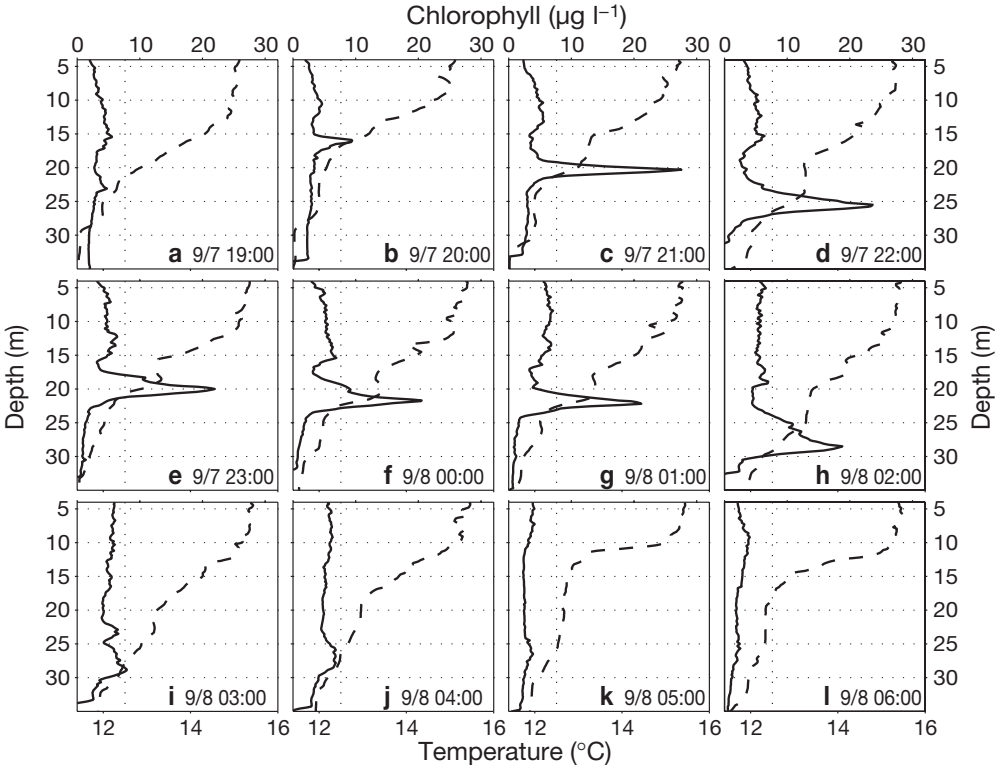

Fig. 9. Relationships between thin phytoplankton layer presence/absence (— chlorophyll [µg l^{-1}]) and thermal profiles (– – temperature [°C]). This sequence of consecutive profiles is from the SeaHorse profiler on 7 and 8 September 2003. The month/day and hour of each profile is noted

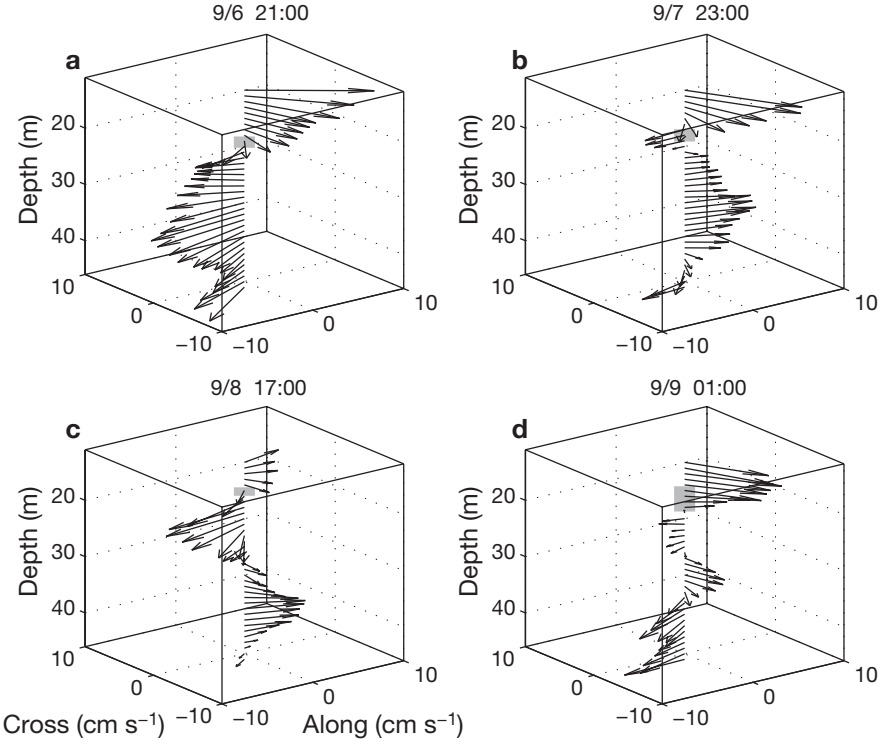

Fig. 10. Examples of the spatial coincidence between thin layers and sharp changes in the direction of horizontal current velocity. Velocity profiles are represented as vectors; thin layer vertical ranges are shown by the shaded bars. The month/day and hour of each example is noted

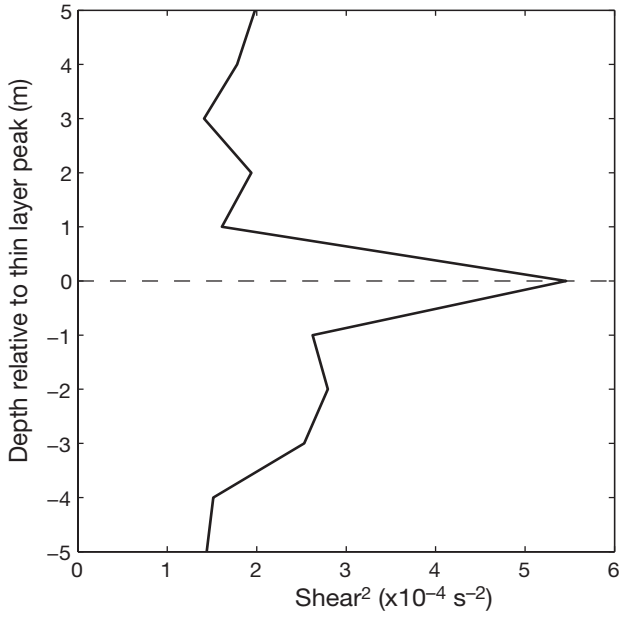

Fig. 11. Median shear squared profile computed in the layer frame of reference (0 m is the center of the thin layer) from all velocity profiles coincident with SeaHorse thin layer profiles (n = 36)

Localized stability for thin layer formation and persistence is indicated by the association of the thin layers with local enhancement of the vertical temperature gradient, i.e. steps in the thermocline.

The thin layer variability we observed by moored profilers occurred within a very dynamic setting in which 2 frontal zones developed. Satellite and *in situ* observations described the processes that created fronts around the profiler moorings. Early in the profiler deployment period, much of the bay was flushed by relatively warm, fresh, low chlorophyll waters. This front was mapped by AUV to show the profilers in the frontal zone, and the satellite data show that this front remained over the profiler mooring site until the first thin layers were observed on 6 September. Satellite data also show that the nature of the frontal zone changed significantly when an upwelling filament flowed immediately west of the profiler mooring. Radar remote sensing showed that this was a convergent front. Although the fronts were very different in nature, phytoplankton thin layers were observed during the presence of both fronts. We consider the key influences of these fronts to include phytoplankton patchiness from which thin layers can be created, and circulation dynamics in the frontal zones that determined the shear patterns acting upon the phytoplankton patches. Both fronts were of a type commonly generated in coastal upwelling systems. Therefore, we hypothesize that thin layer generation in coastal upwelling system fronts may be a commonly occurring process in these systems.

By influencing the distributions and ecology of phytoplankton, development of thin phytoplankton layers has implications for fundamental aspects of marine ecology. By influencing the vertical distribution of biomass relative to the light and nutrient fields, thin layers influence primary productivity. Through the aggregation of biomass in narrow vertical zones, thin phytoplankton layers impact plankton community structure and trophic transfer. The efficiency of trophic transfer, in turn, influences important plankton ecological processes such as survival of zooplankton and fish larvae that require dense prey, and transfer of toxins into the food web from toxin-producing species. While thin layers are important to understand in coastal marine ecological research, this research area is challenging because of the small vertical scales over which thin layers occur, and the rapid environmental changes that are intrinsic to dynamic coastal ocean environments. Previous studies of thin layer ecology in East Sound, a small fjord in the Pacific Northwest, have emphasized the requirement for multidisciplinary observations from regional scale to small vertical scales (Dekshenieks et al. 2001, Rines et al. 2002, McManus et al. 2003). Studies of phytoplankton ecology in Monterey Bay also demonstrate the need for multi-scale, multidisciplinary observation (Ryan et al. 2005a,b, J. P. Ryan unpubl. data), and this thin layer study in Monterey Bay also emphasizes this requirement. Future studies will benefit from synoptic mapping of frontal zones when thin layers are present. Thus real-time data transfer from moorings to shore and event response capability, e.g. launching an AUV mapping mission, will help advance this challenging research area of coastal oceanography.

Acknowledgements. This research was supported in part by the David and Lucile Packard Foundation though MBARI and a grant to the Partnership for Interdisciplinary Studies of Coastal Oceans (PISCO), in part by NASA grant NAG5-12692 (J.P.R. and F.P.C.), and in part by ONR grants N00014-04-1-0311 (J.P.R.) and N000140310267 (M.A.M.). We thank M. Kelley, P. Coenen, and A. Hamilton for profiler mooring deployment efforts, and G. Friederich and M. Harlan for drifter deployment efforts. Thanks to P. McEnaney for processing of the SAR imagery, to R. Kudela for the high-resolution climatological SeaWiFS data in Fig. 1b, and to C. Paull for the bottom pressure record used for description of tidal variation. Sponsorship by NASA's Mission to Planet Earth Program, the SeaWiFS Project (Code 970.2), and the Distributed Active Archive Center (DAAC; Code 902) at the NASA Goddard Space Flight Center made the production and distribution, respectively, of SeaWiFS data possible. MODIS data were acquired as part of the NASA Earth Science Enterprise, algorithms were developed by the MODIS Science Teams, and the data were processed, archived, and distributed through efforts of the MODIS Adaptive Processing System (MODAPS) and Goddard DAAC. SAR images were obtained from the Alaska Satellite Facility (ASF) and projected with software developed by ASF.

LITERATURE CITED

Barber RT, Smith RL (1981) Coastal upwelling ecosystems. In: Longhurst AR (ed) Analysis of marine ecosystems. Academic Press, London, p 31–68

Cowles TJ, Desiderio RA, Neuer S (1993) *In situ* characterization of phytoplankton from vertical profiles of fluorescence emission spectra. Mar Biol 115:217–222

Cowles TJ, Desiderio RA, Carr ME (1998) Small-scale planktonic structure: persistence and trophic consequences. Oceanography 11:4–9

Dekshenieks MM, Donaghay PL, Sullivan JM, Rines JEB, Osborn TR, Twardowski MS (2001) Temporal and spatial occurrence of thin phytoplankton layers in relation to physical processes. Mar Ecol Prog Ser 223:61–71

Donaghay PL, Rines HM, Sieburth JM (1992) Simultaneous sampling of fine scale biological, chemical, and physical structure in stratified waters. Adv Limnol 36: 97–108

Donaghay PL, Sullivan JM, Rines JE, Graff J, Hanson AK, Holliday DV (2006) The importance of swimming behavior in controlling the formation, maintenance and dissipation of thin optical layers. EOS Trans Am Geophys Union 87(36)

Eckart C (1948) An analysis of the stirring and mixing processes in incompressible fluids. J Mar Res 7:265–275

Franks PJS (1995) Thin layers of phytoplankton: a model of formation by near-inertial wave shear. Deep-Sea Res Part I 42:75–91

Johnson PJ, Donaghay PL, Small EB, Sieburth JM (1995) Ultrastructure and ecology of *Perispira ovum* (Ciliophora: Litostomatea): an aerobic planktonic ciliate that sequesters the chloroplasts, mitochondria and paramylon of *Euglena proxima* in a micro-oxic habitat. J Eukaryot Microbiol 422:323–335

Kamykowski D (1974) Possible interactions between phytoplankton and semidiurnal internal tides. J Mar Res 32: 67–89

Koukaras K, Nikolaidis G (2004) Dinophysis blooms in Greek coastal waters (Thermaikos Gulf, NW Aegean Sea). J Plankton Res 26:445–457

Lasker R (1975) Field criteria for the survival of anchovy larvae: the relation between inshore chlorophyll maximum layers and successful first feeding larvae. Fish Bull US 73: 847–855

McManus MA, Alldredge AL, Barnard AH, Boss E and 21 others (2003) Characteristics, distribution and persistence of thin layers over a 48 hour period. Mar Ecol Prog Ser 261: 1–19

McManus MA, Cheriton OM, Drake PJ, Holliday DV, Greenlaw CE, Storlazzi CD, Donaghay PL (2005) Effects of physical processes on structure and transport of thin zooplankton layers in the coastal ocean. Mar Ecol Prog Ser 301:199–215

Mullin MM, Brooks ER (1976) Some consequences of distributional heterogeneity of phytoplankton and zooplankton. Limnol Oceanogr 21:784–796

Paduan JD, Graber HC (1997) Introduction to high frequency radar: reality and myth. Oceanography 10:36–39

Paduan JD, Rosenfeld LK (1996) Remotely sensed surface currents in Monterey Bay from shore-based HF radar (CODAR). J Geophys Res 101:20669–20686

Paduan JD, Kim KC, Cook MS, Chavez FP (2006) Calibration and validation of direction-finding high frequency radar ocean surface current observations. IEEE J Ocean Eng 31(4):862–875

Pennington JT, Chavez FP (2000) Seasonal fluctuations of temperature, salinity, nitrate, chlorophyll and primary production at station H3/M1 over 1989–1996 in Monterey Bay, California. Deep-Sea Res II 47:947–973

Petruncio ET, Rosenfeld LK, Paduan JD (1998) Observations of the internal tide in Monterey Canyon. J Phys Oceanogr 28:1873–1903

Ramp SR, Paduan JD, Shulman I, Kindle J, Barr FL, Chavez FP (2005) Observations of upwelling and relaxation events in the northern Monterey Bay during August 2000. J Geophys Res 110:C07013

Reid JL, Roden GI, Wyllie JG (1958) Studies of the California Current System. Calif Coop Ocean Fish Investig Rep 6:27–56

Rines JEB, Donaghay PL, Dekshenieks MM, Sullivan JM, Twardowski MS (2002) Thin layers and camouflage: hidden *Pseudo-nitzschia* spp. (Bacillariophyceae) populations in a fjord in the San Juan Islands, Washington, USA. Mar Ecol Prog Ser 225:123–137

Rosenfeld LK, Schwing FB, Garfield N, Tracy DE (1994) Bifurcated flow from an upwelling center: a cold water source for Monterey Bay. Cont Shelf Res 14:931–964

Ryan JP, Dierssen HM, Kudela RM, Scholin CA and 6 others (2005a) Coastal ocean physics and red tides: an example from Monterey Bay, California. Oceanography 18:246–255

Ryan JP, Chavez FP, Bellingham JG (2005b) Physical-biological coupling in Monterey Bay, California: topographic influences on phytoplankton ecology. Mar Ecol Prog Ser 287:23–32

Ryther JH (1969) Photosynthesis and fish production in the sea. Science 166:72–76

Thompson DR, Gasparovic RF (1986) Intensity modulation in SAR images of internal waves. Nature 320:345–347

Editorial responsibility: Alain Vézina, Dartmouth, Canada

Submitted: February 27, 2007; Accepted: August 28, 2007
Proofs received from author(s): January 17, 2008